bioRxiv preprint doi: https://doi.org/10.1101/012583; this version posted December 12, 2014. The copyright holder for this preprint (which was not certified by peer review) is the author/funder, who has granted bioRxiv a license to display the preprint in perpetuity. It is made available under aCC-BY-NC-ND 4.0 International license.

Title: Pre-synaptic modulation of afferent feedback in the macaque spinal cord does not modulate with cycles of peripheral oscillations around 10 Hz

Running title: Lack of rapid modulation in pre-synaptic inhibition

Authors: Ferran Galán and Stuart N. Baker

Affiliation: Institute of Neuroscience, Newcastle University, Newcastle upon Tyne, NE2 4HH.

Key words: primary afferent depolarization, pre-synaptic inhibition, tremor.

Number of words: 5185 (excluding references and figure legends)

Correspondence should be addressed to:

Prof Stuart Baker
Institute of Neuroscience,
Henry Wellcome Building
The Medical School
Framlington Place
Newcastle upon Tyne
NE2 4HH
UK
Telephone: +44 (0) 191 208 3271
Fax: +44(0) 191 208 8206
stuart.baker@ncl.ac.uk

bioRxiv preprint doi: https://doi.org/10.1101/012583; this version posted December 12, 2014. The copyright holder for this preprint (which was not certified by peer review) is the author/funder, who has granted bioRxiv a license to display the preprint in perpetuity. It is made available under aCC-BY-NC-ND 4.0 International license.

KEY POINTS

- Presynaptic inhibition of afferent feedback is known to modulate during voluntary movements

- Spinal interneuron circuits have previously been demonstrated to modulate activity with the phase of ~10 Hz physiological tremor, in a manner which promotes cancellation of oscillations and hence tremor reduction

- In this study, we investigated whether afferent pre-synaptic inhibition could also modulate on the faster timescale of tremor oscillations

- Although we found evidence for task-dependent modulation of pre-synaptic inhibition (a timescale of around 1 s), there was no evidence for modulation with the phase of tremor (timescale around 100 ms)

- The results suggest that pre-synaptic inhibition modulates afferent feedback gain dependent on overall motor state, rather than in response to moment-by-moment fluctuations in output

(116 words)

bioRxiv preprint doi: https://doi.org/10.1101/012583; this version posted December 12, 2014. The copyright holder for this preprint (which was not certified by peer review) is the author/funder, who has granted bioRxiv a license to display the preprint in perpetuity. It is made available under aCC-BY-NC-ND 4.0 International license.

ABSTRACT

Spinal interneurons are partially phase-locked to physiological tremor around 10Hz. The phase of spinal activity is approximately opposite to descending drive to motoneurons, leading to partial phase cancellation and tremor reduction. Pre-synaptic inhibition of afferent feedback has been demonstrated to increase during voluntary movements, but it is not known whether it tracks more rapid fluctuations in output such as during tremor.

In this study, we recorded dorsal root potentials (DRPs) from the C8 and T1 roots in two macaque monkeys following intra-spinal micro-stimulation (1-3Hz, 30-100μA), whilst the animals performed an index finger flexion task which elicited substantial peripheral oscillations around 10Hz. Forty one responses were identified with latency <5ms; these were narrow (mean width 0.59 ms), and likely resulted from antidromic activation of afferents following stimulation near terminals. Significant modulation during task performance occurred in 16/41 responses, reflecting terminal excitability changes generated by pre-synaptic inhibition (Wall's excitability test).

Stimuli falling during large-amplitude 8-12Hz oscillations in finger acceleration were extracted, and sub-averages of DRPs constructed for stimuli delivered at different oscillation phases. Although some apparent phase-dependent modulation was seen, this was not above the level expected by chance fluctuation.

We conclude that although pre-synaptic inhibition modulates over the timescale of a voluntary movement (around one second), it does not follow more rapid changes in motor output. This suggests that pre-synaptic inhibition is not part of the spinal systems for tremor reduction described previously, and that it plays a role in overall – but not moment-by-moment – regulation of feedback gain.

(246 words)

bioRxiv preprint doi: https://doi.org/10.1101/012583; this version posted December 12, 2014. The copyright holder for this preprint (which was not certified by peer review) is the author/funder, who has granted bioRxiv a license to display the preprint in perpetuity. It is made available under aCC-BY-NC-ND 4.0 International license.

INTRODUCTION

Physiological tremor is produced by multiple interacting mechanisms. These include mechanical resonance of limb articulations (Marsden *et al.*, 1969), and oscillations in the stretch reflex loop consequent on the peripheral conduction delays (Lippold, 1970). However, there is also a centrally generated component in the 8-12Hz frequency range, as its frequency is unaltered by manoeuvers such as loading the limb, which alter mechanical and reflex resonant frequencies (Elble & Randall, 1978). In addition to physiological tremor, other situations can produce ~10Hz oscillations of the periphery, which also appear to have a central component. These include shivering (Stuart *et al.*, 1966), the cat 'paw shake' response (Hoy *et al.*, 1985) and finger acceleration discontinuities during the execution of slow finger movements (Vallbo & Wessberg, 1993). Studies assessing slow finger movements in non-human primates have found coherence at ~10Hz between acceleration and the activity of multiple motor structures during both active movements and periods of steady holding (Williams *et al.*, 2010), suggesting that physiological tremor and discontinuities during slow finger movements reflect the same underlying phenomenon.

Interestingly, motor cortical oscillations at ~10Hz are not coherent with muscle activity in this range during steady holding (Conway *et al.*, 1995; Baker *et al.*, 1997; Salenius *et al.*, 1997; Baker *et al.*, 2003), despite their passage down the corticospinal tract (Baker *et al.*, 2003). Based on these observations, we have previously suggested the existence of an active neural filter, which removes ~10Hz components from the input to motoneurons (Baker *et al.*, 2003; Williams & Baker, 2009; Williams *et al.*, 2010). A system which removed or cancelled ~10Hz oscillations could be important in the reduction of tremor. In some circumstances, minor maladjustment of such a system could generate 10Hz oscillations, thereby producing a central tremor component.

Work in anaesthetized animals has previously demonstrated the existence of ~10Hz oscillations in spinal circuits (Lidierth & Wall, 1996). Oscillations survive afferent section (Lidierth & Wall, 1996), indicating that they are generated centrally rather than by a peripheral feedback loop. Oscillations are intrinsic to the cord, but controlled by descending pathways, as they are larger

bioRxiv preprint doi: https://doi.org/10.1101/012583; this version posted December 12, 2014. The copyright holder for this preprint (which was not certified by peer review) is the author/funder, who has granted bioRxiv a license to display the preprint in perpetuity. It is made available under aCC-BY-NC-ND 4.0 International license.

following cord section (Lidierth & Wall, 1996). Additionally, the cat paw shake response survives spinal transection (Koshland & Smith, 1989), suggesting that is based on rhythmic spinal circuits. When investigating neural systems contributing to ~10Hz discontinuities during slow finger movements, we found evidence that a wide range of structures were involved. However, the phase relationship between neural activity and finger acceleration was inverted for spinal field potentials, possibly pointing to spinal circuits as the most likely location of a putative 'tremor filter' (Williams *et al.*, 2010).

Spinal networks could influence motoneurons by multiple possible pathways, most obviously by excitatory or inhibitory synapses on the motoneurons themselves. One known instance of such a direct synaptic effect is Renshaw cell recurrent inhibition, which previous work has shown can partially cancel ~10Hz components in motoneuron input (Williams & Baker, 2009). However, spontaneous oscillations in the cord are also synchronized with similar oscillations in dorsal root potentials (Lidierth & Wall, 1996), and are associated with primary afferent depolarization (PAD) (Manjarrez *et al.*, 2000) which reflects pre-synaptic inhibition of afferent input. This led us to hypothesize that presynaptic inhibition might also be configured to modulate with the ~10 Hz oscillations of tremor. By modulating afferent input, such oscillations in presynaptic inhibition could alter drive to motoneurons just as effectively as direct synapses to the motoneuron dendrites. This might have particular advantages in cancelling oscillations in afferent input caused by resonance in the stretch reflex arc (see Fig. 1a).

Pre-synaptic inhibition modulates during voluntary movements (Hultborn *et al.*, 1987; Seki *et al.*, 2003), and can suppress motor oscillations during forelimb movement (Fink *et al.*, 2014). Descending control over pre-synaptic inhibition is exerted by the corticospinal (Rudomin *et al.*, 1983; Rudomin *et al.*, 1986; Iles & Pisini, 1992; Meunier & Pierrot-Deseilligny, 1998) and reticulospinal tract (Rudomin *et al.*, 1983; Rudomin *et al.*, 1986). Activity in both motor cortex and reticular formation synchronizes with tremor during slow finger movements (Williams *et al.*, 2010), such that tremor-related modulation of presynaptic inhibition is a reasonable hypothesis.

bioRxiv preprint doi: https://doi.org/10.1101/012583; this version posted December 12, 2014. The copyright holder for this preprint (which was not certified by peer review) is the author/funder, who has granted bioRxiv a license to display the preprint in perpetuity. It is made available under aCC-BY-NC-ND 4.0 International license.

In this report, we used a new technique that allowed recordings from a mixed population of muscle and cutaneous afferents in awake behaving primates, and investigated whether afferent axon terminal excitability modulates during performance of a slow index finger flexion task, and with the cycles of physiological tremor which are prominent in such a task. Surprisingly, although robust modulation over the second-to-second timescale of task performance was regularly seen, our data contained no evidence for faster modulation of pre-synaptic inhibition during the tremor cycle. We conclude that pre-synaptic inhibition may act as a less temporally-precise gate for afferent inflow, but does not sculpt sensory input and its reflex consequences over timescales comparable to endogenous oscillations in motor output.

METHODS

Behavioural task

Two female *Macaca mulatta* monkeys (denoted I and V) were trained to perform a finger flexion task for food reward, similar to that used in our previous work (Williams *et al.*, 2009; Williams *et al.*, 2010; Soteropoulos *et al.*, 2012). The index finger of the right hand was inserted into a narrow tube, which restricted movement to the metacarpophalangeal (MCP) joint. The tube was attached to a lever that rotated coaxially with the MCP joint; a motor exerted torque in a direction to oppose flexion. Lever angular displacement was sensed by an optical encoder and fed back to the animal via a cursor on a computer screen. A displacement of 0° indicated the neutral position, where the finger was in the same plane as the palm. Positive angles denoted finger flexion. During each trial the palm and digits 1, 3, 4, and 5 lay horizontally against a flat surface and the elbow and upper arm were held in a sleeve. The contralateral arm was unrestrained.

For both animals, a trial commenced when a rectangular target appeared at 8° displacement. The animal moved the cursor into this target, which then moved over a linearly increasing displacement (ramp). In monkey I, the ramp phase lasted 1.5 s, with final displacement 20°; the trial was completed at the end of the ramp phase. In monkey V, the ramp phase lasted 2 s, with final displacement 16°; at the end of the ramp, there was a hold phase of constant target

bioRxiv preprint doi: https://doi.org/10.1101/012583; this version posted December 12, 2014. The copyright holder for this preprint (which was not certified by peer review) is the author/funder, who has granted bioRxiv a license to display the preprint in perpetuity. It is made available under aCC-BY-NC-ND 4.0 International license.

displacement lasting 1 s. Maintenance of the cursor within the target (allowed error ±1.4°) led to a food reward. An accelerometer attached to the lever measured movement discontinuities during the target ramp (band-pass, 1–100 Hz).

Surgical preparation

Following training, both animals were implanted under general anaesthesia (3.0–5.0% sevoflurane inhalation, intravenous infusion of 0.025 $mg \cdot kg^{-1} \cdot h^{-1}$ alfentanil) and aseptic conditions with a stainless steel headpiece for head fixation. After an appropriate recovery period, a further surgery implanted a spinal chamber over a laminectomy spanning vertebrae C5-C7, together with a bipolar cuff electrode on the C8 (monkey I) or T1 (monkey V) dorsal root adjacent to the cord. This cylindrical cuff electrode was modelled on those commonly used for peripheral nerve stimulation and recording. It was manufactured from flexible medical-grade silicone polymer to have an internal diameter of 4.0 mm and length 10 mm. The cuff contained two platinum electrodes which ran around the internal circumference (electrode width 1.0 mm, separation 3.5 mm), and were spot-welded to Teflon-insulated stainless steel wire (wire diameter 150 μm). The dorsal root was inserted into the cuff via a slit along the length of the cuff, which was then closed using two silk sutures which ran around the outside. Cuff placement was made possible by the fact that in monkey the C8/T1 roots run parallel to the cord for some distance before turning to exit the facet joint. This displacement between spinal segment and equivalent vertebra is much more marked in monkey than in man, where roots do not run parallel to the cord in this way until the mid-throracic level. The wires were run over the lateral mass and then up the side of the chamber, where they terminated in a connector. Both wires and connector were covered in dental acrylic for protection.

A full program of post-operative analgesia followed all surgical procedures. All procedures were carried out under the authority of licenses issued by the UK Home Office under the Animals (Scientific Procedures) Act (1986) and were approved by the Animal Welfare and Ethical Review Board of Newcastle University.

bioRxiv preprint doi: https://doi.org/10.1101/012583; this version posted December 12, 2014. The copyright holder for this preprint (which was not certified by peer review) is the author/funder, who has granted bioRxiv a license to display the preprint in perpetuity. It is made available under aCC-BY-NC-ND 4.0 International license.

Recordings

During task performance both head and spinal implants were fixed to the primate chair and a microdrive was interfaced to the spinal chamber via an X-Y positioning stage. Differential recordings from the contacts of the dorsal root cuff electrodes yielded the dorsal root potential (DRP, band pass 3 Hz-2 kHz, gain 50 K). Intraspinal microstimulation (ISMS) (bipolar pulses, 0.07-0.1 ms per phase, 1-3 Hz, 30-100 µA) was delivered through a tungsten microelectrode (impedance 1 MΩ) inserted into the spinal grey matter at a location which evoked responses in the DRP (see Fig. 1). Stimulus intensity was set to yield response amplitudes around half of the maximum. Stimulus timing was controlled by a 1401 interface (CED Ltd, Cambridge, UK), which also recorded DRP (sampling rate 20 kHz), lever position and acceleration (sampling rate 1 kHz) and task markers to disk for later off-line analysis.

Dorsal root responses following ISMS had a complex profile. In order to clarify the origin of the different components, we compared them with responses following median nerve stimulation (1ms bipolar pulses, 1-3 Hz, 0.4-1.8 mA applied to surface electrodes at the wrist) in both the dorsal root cuff and the spinal cord (recorded by a tungsten microelectrode as above, band pass 1 Hz-5 kHz, gain 2 K, sampling rate 10 kHz; Fig. 2).

Modulation of ISMS evoked responses at dorsal root

Evoked responses in the DRP following ISMS were first determined by averaging triggered by all stimuli delivered to a given spinal site. This allowed estimation of the peak-to-peak amplitude of each component, measured over a time window selected manually. The latency was estimated from the time of the first peak of that component.

To estimate the task-dependent modulation of responses, trials were first aligned to the end of the ramp phase of the task. Stimuli were then sorted depending on when they had occurred relative to this alignment point, into 26 non-overlapping bins, each 200 ms wide, spanning from 3 s before to 2 s after the end of the ramp. Selective averages were compiled of stimuli in each bin, and

bioRxiv preprint doi: https://doi.org/10.1101/012583; this version posted December 12, 2014. The copyright holder for this preprint (which was not certified by peer review) is the author/funder, who has granted bioRxiv a license to display the preprint in perpetuity. It is made available under aCC-BY-NC-ND 4.0 International license.

amplitude measured from each average using the time window defined from the all-stimulus average.

To estimate how evoked responses modulated with tremor phase, stimuli were first selected using two criteria. It is known that peripheral oscillations are stronger during periods of finger movement (which motivated our use of a task incorporating a ramp phase). Accordingly, the finger lever velocity V was estimated over a window prior to the stimulus at time T as

$$V(t) = \frac{x(T) - x(T-\tau)}{\tau} \qquad \text{(Eq. 1)}$$

Where x represents the lever displacement, and the window length τ was set to 100 ms. The amplitude spectrum of the lever acceleration was estimated over a window prior to the stimulus at time t using non-symmetric causal wavelets as described in (Mitchell *et al.*, 2007). In brief, the wavelet W at frequency f was defined as the product of an alpha function with peak $0.8/f$ before the stimulus, with a complex sinusoid:

$$W^f(t) = -\frac{5ft}{4} e^{\left(2\pi f t i + \frac{5ft}{4}\right)} \qquad \text{(Eq. 2)}$$

For a given frequency f, a section of accelerometer signal S was extracted lasting seven oscillation periods prior to the stimulus at time T. The dot-product of the accelerometer signal S with the wavelet W^f was found:

$$D^f = \int_{t=-7/f}^{0} W^f(t) S(t+T) dt \qquad \text{(Eq. 3)}$$

The amplitude A and phase φ were measured as:

$$A^f = \left| D^f \right|$$

bioRxiv preprint doi: https://doi.org/10.1101/012583; this version posted December 12, 2014. The copyright holder for this preprint (which was not certified by peer review) is the author/funder, who has granted bioRxiv a license to display the preprint in perpetuity. It is made available under aCC-BY-NC-ND 4.0 International license.

$$\phi^f = arctan\left(\frac{Im\{D^f\}}{Re\{D^f\}}\right) \quad \text{(Eq. 4)}$$

Only stimuli with V>15 °/s and which had the bin with largest spectral power lying within the 8-12 Hz range were included for subsequent analysis of tremor modulation. Note that using these criteria, stimuli falling in unsuccessful trials (e.g. where the animal strayed outside the imposed limits on tracking performance towards the end of a trial) were able to be used as well as those during successful task performance.

Stimuli which survived this pre-selection were then grouped by the phase of on-going lever acceleration oscillations in which they occurred, using eight equally-sized bins from 0 to 2π. DRP averages were then compiled selectively from stimuli in each bin, and response amplitude measured for each sub-average as for the determination of task modulation.

Plots of response amplitude versus bin number often showed complex patterns of modulation, for both task and phase dependent modulation. We developed a simple summary measure, which quantified the overall extent of this modulation in a single number. First, we computed a raw modulation index from the experimental data, I_{exp}, as

$$I_{exp} = \sum_{n=1}^{N} |A_n - \bar{A}| \quad \text{(Eq. 5)}$$

Where A_n is the response amplitude measured in bin n. The number of bins N was 26 for task modulation and 8 for tremor. The mean response $\bar{A}$ was calculated as:

$$\bar{A} = \frac{1}{N}\sum_{n=1}^{N} A_n \quad \text{(Eq. 6)}$$

The measure I quantifies how much single bin responses deviate from the average response, but it is difficult to interpret the scale of this number. Accordingly, we generated surrogate datasets, which estimated how great I would be, on the null hypothesis of no response modulation above

bioRxiv preprint doi: https://doi.org/10.1101/012583; this version posted December 12, 2014. The copyright holder for this preprint (which was not certified by peer review) is the author/funder, who has granted bioRxiv a license to display the preprint in perpetuity. It is made available under aCC-BY-NC-ND 4.0 International license.

that expected by chance fluctuations. Surrogates were compiled by randomly shuffling bin assignments of individual stimuli; for a given bin, the number of stimuli assigned to it was fixed equal to the number in the experimentally determined dataset. Sub-averages were compiled for the surrogate data, and the measure *I* recompiled. This was repeated 500 times, using different random assignments of stimuli to bins. The mean $\bar{I}$ and standard deviation σ_I of the surrogate values of *I* was found, allowing us to compute a normalised modulation index (NMI_{exp}) as:

$$NMI_{exp} = \frac{I_{exp} - \bar{I}}{\sigma_I} \qquad \text{(Eq. 7)}$$

If I_{exp} exceeded the 95th percentile of the surrogate values of *I*, the modulation was considered to be statistically significant (P<0.05).

To interpret the scale of tremor modulation in the 8-12 Hz range further and be able to compare it with other frequency ranges, we combined data across recording sites in two ways, estimating both the count *C* of significantly tremor-modulating responses, and also the mean modulation index $\overline{NMI}$ across all sites. Surrogate measures of C and $\overline{NMI}$ were generated by counting or averaging over one surrogate value of *I* per site; this was repeated 500 times with different randomly generated surrogates. If C_{exp} and $\overline{NMI}_{exp}$ from the experimental data exceeded the 95th percentile of the surrogate values, they were considered to be statistically significant (P<0.05). This whole procedure was repeated for frequencies between 6 and 50 Hz.

Identification of task-dependent modulation patterns of ISMS evoked responses at dorsal root

We were interested to determine whether responses with a significant task-dependent modulation from different spinal sites could be grouped into a smaller number of representative profiles. Profiles were accordingly subjected to unsupervised *k*-means clustering, using the correlation between profiles of amplitude versus bin number as the metric of pairwise distance. The number of identified patterns (=number of clusters, s) was chosen by maximizing the relatedness of the

bioRxiv preprint doi: https://doi.org/10.1101/012583; this version posted December 12, 2014. The copyright holder for this preprint (which was not certified by peer review) is the author/funder, who has granted bioRxiv a license to display the preprint in perpetuity. It is made available under aCC-BY-NC-ND 4.0 International license.

modulating responses across solutions for s=1..10. Response relatedness was estimated using the intra-cluster correlation coefficient:

$$ICC(s) = \frac{\overline{Corr}_{within}}{\overline{Corr}_{within} + \overline{Corr}_{between}} \quad \text{(Eq. 8)}$$

Where $\overline{Corr}_{within}$ is the average squared correlation within clusters, and $\overline{Corr}_{between}$ is the average squared correlation between clusters. Given a clustering solution s with clusters indexed by c or d=1..s, and each cluster containing n_c responses Resp^c_j (j=1..n_c), $\overline{Corr}_{within}$ and $\overline{Corr}_{between}$ were calculated as:

$$\overline{Corr}_{within} = \frac{1}{n_c s} \sum_{c=1}^{s} \sum_{j=1}^{n_c} Corr(Resp_j^c, Centroid_c)$$

$$\overline{Corr}_{between} = \frac{1}{s^2} \sum_{c=1}^{s} \sum_{d=1}^{s} Corr(Centroid_c, Centroid_d) \quad \text{(Eq. 9)}$$

Where $Corr(Resp_j^c, Centroid_c)$ is the squared correlation between a response $Resp^c_j$ and the centroid of parent cluster, and $Corr(Centroid_c, Centroid_d)$ is the squared correlation between centroids of clusters c and d.

Values of ICC_s close to one reflect solutions where responses are very similar within a cluster, but unrelated to those in another cluster. Estimates of ICC_s were produced using leave-one-out cross-validation, in which each response was correlated with cluster centroids determined after excluding that response from the dataset.

All analysis routines were implemented in the MATLAB package (The MathWorks Inc, Natick, MA, USA).

bioRxiv preprint doi: https://doi.org/10.1101/012583; this version posted December 12, 2014. The copyright holder for this preprint (which was not certified by peer review) is the author/funder, who has granted bioRxiv a license to display the preprint in perpetuity. It is made available under aCC-BY-NC-ND 4.0 International license.

RESULTS

Responses evoked in Dorsal Root Recordings by ISMS

Results were available from stimulation at a total of 21 spinal sites (8 monkey I, 13 monkey V). At each site, between 392 and 29516 stimuli were delivered, whilst the animal performed between 20 and 161 successful trials of the task.

Figure 1B illustrates typical raw data from an experiment, and Fig. 1C shows the averaged DRP evoked by the ISMS (stimulus intensity 65 μA). A complex waveform was visible in this average, reflecting multiple components of the response which are identified by the grey shading labelled with lower case letters.

Figure 1D shows how the different parts of the response from Fig. 1C modulated with task performance. Each trace shows the amplitude of one component as a function of time during the task (see averaged lever displacement beneath as a reference); traces illustrate both averaged amplitude (thick lines) and the corresponding standard error of the mean (thin lines). The three earliest responses (a, b, c) exhibited only chance fluctuations, and the corresponding NMI values were below the 95th percentile of those in surrogate datasets (experimental / 95th centile surrogate NMI: a, 1.2/1.8; b, 1.2/1.7; c, 1.1/1.7). By contrast, both later responses had NMI outside those expected by chance from surrogate data (d, 2.4/1.6; e, 3.4/1.7), indicating a significant modulation with task.

Across all 21 spinal sites which were stimulated, we identified a total of 88 distinct responses in the DRP, 57 of which (65%) modulated significantly with the task. In order to provide some insight into the physiological mechanisms generating the different response components, Fig. 1E plots their width (peak-trough time) versus latency (time of earliest peak/trough); components which modulated significantly with task are identified by empty circles. It is clear that there are three broad classes of response. The earliest components (latency <5 ms) were narrow (width 0.59±0.05 ms, mean ± SEM), and contained a mixture of modulating (16/41) and non-modulating

bioRxiv preprint doi: https://doi.org/10.1101/012583; this version posted December 12, 2014. The copyright holder for this preprint (which was not certified by peer review) is the author/funder, who has granted bioRxiv a license to display the preprint in perpetuity. It is made available under aCC-BY-NC-ND 4.0 International license.

(25/41) effects. These are most likely to reflect antidromic action potentials generated by direct stimulation of afferent axons within the cord. Such effects could exhibit a task relationship if the stimulating electrode was close to axon terminals, and those terminals were depolarized by axo-axonic synapses mediating primary afferent depolarization (PAD; Wall, 1958), thereby modulating their excitability to the stimulus. Instances where these early responses did not modulate with task could reflect either terminals which do not receive task-dependent PAD, or situations where the stimulating electrode activated stem axons, distant from the terminals and hence with a constant level of excitability.

There appeared to be two later clusters of responses, with mean latencies of 8.1 ms and 18.1 ms. These showed a greater incidence of task-dependent modulation (22/24 and 19/23 responses respectively); both groupings of response were broader (widths 3.3±0.1 ms and 4.1±0.1 ms respectively). One possible cause for these effects could be PAD elicited in afferent axon terminals by activation of spinal neurons following the stimulus, and passively conducted to the dorsal root recording site (Wall, 1958).

Comparison with Responses evoked in Dorsal Root Recordings by Peripheral Nerve Stimulation

Further insight into the mechanisms generating the later DRPs described above was provided by examining the responses to peripheral nerve stimulation (Fig. 2A). Figure 2B shows the average response after stimulation of the median nerve at the wrist, at an intensity 1.4 mA, for a single recording session. The DRP recording showed a compound volley, which has a first peak latency 3.9 ms after the stimulus. This contained multiple sharp components, presumably reflecting different axons of different conduction velocities, and was followed by a slower potential (width peak-to-peak 1.0 ms), with first peak at 10.1 ms after the stimulus. Such a potential is consistent with previous reports of PAD following peripheral nerve stimulation.

Figure 2C illustrates that this later potential modulated strongly with task performance, indicating that the excitability of neural populations mediating PAD changed in a task-dependent manner.

bioRxiv preprint doi: https://doi.org/10.1101/012583; this version posted December 12, 2014. The copyright holder for this preprint (which was not certified by peer review) is the author/funder, who has granted bioRxiv a license to display the preprint in perpetuity. It is made available under aCC-BY-NC-ND 4.0 International license.

Significant task-dependent modulation of a potential similar to that seen in Fig. 2B was observed in 3/4 recording sessions where median nerve stimulation was tested (NMI values 12.3, 5.0 and 17.0).

In these three sessions, the average latency difference between the earliest afferent volley and the later PAD potential was 5.1±0.58 ms; the width of the later PAD potential was 1.1±0.05 ms (both mean±SEM). The latency is comparable to the later potentials seen following ISMS in Fig. 1E, although those elicited by afferent input are considerably shorter, possibly related to the prior activation of the terminals by the afferent volley. The responses to median nerve stimulation therefore seem broadly to support the idea that the later responses to ISMS reflect PAD elicited by activation of spinal neurons.

Patterns in the Task-dependent Modulation of ISMS-Evoked Dorsal Root Responses

We used a k-means clustering approach to examine whether there were any repeatable patterns in the task modulation profiles of the short-latency (<5 ms) ISMS responses from different sites (see Methods). A plot of the intra-cluster correlation (Fig. 3A) revealed a sharp increase in going from one to two clusters, but then only a small increase as the cluster number was further increased, peaking at four clusters. Figure 3B presents information on the different profiles identified. Of the 16 responses with significant modulation, 7 showed response facilitation during the task ramp phase (MP+), while 5 showed a facilitation just after the ramp phase ended (MP-). The remaining two clusters appeared to have erratic profiles and were categorized as MP*1 and MP*2 (n=2 sites each). Averaged lever displacement traces are shown at the bottom in Figure 3B, and make clear that there were differences in the temporal profile of task performance between the two animals. Interestingly, the modulation profiles MP+, MP*1 and MP*2 all occurred in monkey V, whereas MP- profiles all occurred in monkey I, suggesting that individual differences in the task and its performance lay behind the modulation differences. There was no significant difference between the modulation depths of the four patterns (Fig. 3C; P=0.104, Kruskal-Wallis test).

bioRxiv preprint doi: https://doi.org/10.1101/012583; this version posted December 12, 2014. The copyright holder for this preprint (which was not certified by peer review) is the author/funder, who has granted bioRxiv a license to display the preprint in perpetuity. It is made available under aCC-BY-NC-ND 4.0 International license.

Modulation of ISMS Evoked Dorsal Root Responses with Tremor Cycle

Figure 4A illustrates typical raw data from an experiment, marking with vertical dotted lines the stimuli which were included for analysis of tremor modulation based on a linearly increasing lever displacement and a power spectral peak of lever acceleration in the 8-12 Hz range. Figure 4B shows the asymmetric wavelet used to extract amplitude and phase information from the acceleration signal (see Methods). Figure 4C shows two example phase-dependent modulation profiles of responses classified as MP+ and MP- on the basis of task. Each of these had NMI values above those expected by chance from surrogate data, indicating a significant modulation with tremor oscillatory phase at the frequencies illustrated (9 Hz and 10 Hz respectively).

To examine whether this modulation in the ~10 Hz tremor range was above that expected by chance and whether it reflected the specific involvement of presynaptic inhibition in regulating these frequencies, we evaluated the count of significantly modulating responses and the average modulation depth across the 6-50 Hz frequency range (1 Hz resolution; see Methods). This is illustrated in Fig. 4D, for responses which modulated significantly with task; experimental values are shown with bars, together with the 95th percentile of surrogate data with dotted traces. Neither the number of modulating responses, nor the mean modulation index exceeded the bounds expected by chance, at any of the frequencies tested. Figure 4E repeats this analysis for those responses which did not show a significant task-dependent modulation; once again, no significant modulation with tremor was detected.

In the case of the task-modulating responses of Fig. 4D, it is conceivable that pooling responses with different task-modulating profiles has obscured a significant modulation at the sub-population level. To explore this in more detail, we stratified the phase-dependent analysis by considering responses with MP+ and MP- modulating profiles separately (MP*1 and MP*2 were excluded due to their small sample size; n=2 sites each). The count of modulating sites did not rise above the bounds expected by chance for either profile at any frequency (Fig. 4FG, top traces). For the average modulation index in MP- responses, 2/45 frequency bins exceeded the 95th percentile of the surrogate data, at 24 and 25 Hz. However, two or more frequency bins

bioRxiv preprint doi: https://doi.org/10.1101/012583; this version posted December 12, 2014. The copyright holder for this preprint (which was not certified by peer review) is the author/funder, who has granted bioRxiv a license to display the preprint in perpetuity. It is made available under aCC-BY-NC-ND 4.0 International license.

exceed the P<0.05 significance level merely by chance 45% of the time (surrogate distribution). We therefore discount this finding as a statistical fluctuation, and conclude that there is no evidence in our dataset for modulation of the dorsal root responses and phase of peripheral oscillations at any frequency tested.

DISCUSSION

Previous work has demonstrated that pre-synaptic inhibition of cutaneous afferents can modulate in amplitude with different phases of task performance (Seki *et al.*, 2003, 2009), consistent with a role as a 'gate' to control afferent inflow during voluntary movement. Our present results confirm such task-dependent modulation for a presumed mixed population of muscle and cutaneous afferents. However, based on prior work it was not clear whether pre-synaptic inhibition could modify afferent gain on a faster timescale. On the one hand, the earliest reports showed that changes in monosynaptic reflex amplitude could develop within 10 ms, and recover over around 100 ms (Eccles *et al.*, 1961); this work used preparations with reduced body temperature, which would plausibly have slowed the time course of effects. Under barbiturate anaesthesia at physiological temperatures there are spontaneously occurring deflections in cord-dorsum potentials. Monosynaptic reflexes evoked synchronously with these potentials are markedly potentiated, but return to baseline levels within just 30 ms (see Fig. 8 in Manjarrez *et al.*, 2000). Fast timescale modulations in pre-synaptic inhibition therefore seem possible. On the other hand, if pre-synaptic inhibition is elicited by brief trains of stimuli, its duration can be greatly prolonged, with effects often outlasting the stimulus for up to one second (Eccles *et al.*, 1961; Fink *et al.*, 2014). This has been suggested to result from asynchronous release of synaptic transmitter from the axo-axonic contact, or an action on slower metabotropic ($GABA_B$) receptors (Fink *et al.*, 2014). Such actions would seem incompatible with fast modulation. It is not clear where within this spectrum of observations the action of physiological activity should be placed.

The present report demonstrates that, at least in one commonly occurring natural state, pre-synaptic inhibition does not modulate on fast timescales. This negative result assumes special importance in the context of our other findings related to spinal systems and their activity during

bioRxiv preprint doi: https://doi.org/10.1101/012583; this version posted December 12, 2014. The copyright holder for this preprint (which was not certified by peer review) is the author/funder, who has granted bioRxiv a license to display the preprint in perpetuity. It is made available under aCC-BY-NC-ND 4.0 International license.

the ~10 Hz oscillations of physiological tremor. We have shown that cortical, brainstem and spinal interneuronal circuits (including pre-motoneuronal interneurons) all modulate their discharge with the tremor cycle (Williams & Baker, 2009; Williams *et al.*, 2009; Williams *et al.*, 2010). The phase relationship of spinal interneurons appears opposite to that of the supra-spinal centres, permitting partial cancellation of oscillatory activity at the motoneuronal level and reduction of oscillatory output. The different phase relationships appear to arise from different responses to sensory input (Kozelj & Baker, 2014). Given the existence of spinal systems for phase cancelation of oscillations around 10As with any negative result, we must consider whether some aspect of our experimental design prevented us from detecting a modulation. The most powerful argument that this was not the case is that we were able to demonstrate clear modulations in spinal terminal excitability with task performance, consistent with previous work (Seki *et al.*, 2003, 2009). We deliberately used intensities which yielded responses around half-maximal, which should be most sensitive to modulation by excitability changes. Sufficient stimuli were delivered that the signal:noise ratio in response averages was low (Fig. 1C; see small size of error bars of Fig. 1D, 4C), arguing against statistical thresholding leading to us not detecting small modulations.

Recently, Fink *et al.* (2014) were able to investigate the contributions of pre-synaptic inhibition to motor control directly in mice using a genetic approach which destroyed pre-synaptic contacts, identified because they specifically express *Gad2*. During forelimb reaching, these mice show oscillatory movements which seem to result from an excessive afferent reflex gain. It would appear that pre-synaptic inhibition is modulated on relatively crude temporal timescales to mark the transition from postural stabilisation to movement, with attendant switch from a motor set dominated by reflexes to one under descending voluntary command (Seki *et al.*, 2003, 2009). This switch allows high reflex gain during periods of constant output, but prevents reflexes from interfering with active movement. Our results suggest that faster modulations in afferent sensitivity in response to temporal fluctuations in output do not occur.

bioRxiv preprint doi: https://doi.org/10.1101/012583; this version posted December 12, 2014. The copyright holder for this preprint (which was not certified by peer review) is the author/funder, who has granted bioRxiv a license to display the preprint in perpetuity. It is made available under aCC-BY-NC-ND 4.0 International license.

ADDITIONAL INFORMATION

Author contributions

SNB designed the study; SNB and FG carried out the experiments; FG performed data analysis and SNB and FG wrote the manuscript.

Competing interests

None declared.

Funding

This work was supported by the Wellcome Trust.

Acknowledgements

The authors thank Paul Flecknell and Aurelie Thomas for veterinary and anaesthesia assistance, Caroline Fox and Denise Reed for theatre nursing, Terri Jackson for animal care, and Norman Charlton for mechanical workshop support.

bioRxiv preprint doi: https://doi.org/10.1101/012583; this version posted December 12, 2014. The copyright holder for this preprint (which was not certified by peer review) is the author/funder, who has granted bioRxiv a license to display the preprint in perpetuity. It is made available under aCC-BY-NC-ND 4.0 International license.

REFERENCES

Baker SN, Olivier E & Lemon RN. (1997). Coherent oscillations in monkey motor cortex and hand muscle EMG show task-dependent modulation. *J Physiol* **501 (Pt 1),** 225-241.

Baker SN, Pinches EM & Lemon RN. (2003). Synchronization in monkey motor cortex during a precision grip task. II. effect of oscillatory activity on corticospinal output. *J Neurophysiol* **89,** 1941-1953.

Conway BA, Halliday DM, Farmer SF, Shahani U, Maas P, Weir AI & Rosenberg JR. (1995). Synchronization between motor cortex and spinal motoneuronal pool during the performance of a maintained motor task in man. *J Physiol* **489,** 917-924.

Eccles JC, Eccles RM & Magni F. (1961). Central inhibitory action attributable to presynaptic depolarization produced by muscle afferent volleys. *J Physiol* **159,** 147-166.

Elble RJ & Randall JE. (1978). Mechanistic components of normal hand tremor. *Electroencephalography and clinical neurophysiology* **44,** 72-82.

Fink AJ, Croce KR, Huang ZJ, Abbott LF, Jessell TM & Azim E. (2014). Presynaptic inhibition of spinal sensory feedback ensures smooth movement. *Nature* **509,** 43-48.

Hoy MG, Zernicke RF & Smith JL. (1985). Contrasting roles of inertial and muscle moments at knee and ankle during paw-shake response. *Journal of neurophysiology* **54,** 1282-1294.

Hultborn H, Meunier S, Pierrot-Deseilligny E & Shindo M. (1987). Changes in presynaptic inhibition of Ia fibres at the onset of voluntary contraction in man. *The Journal of physiology* **389,** 757-772.

Iles JF & Pisini JV. (1992). Cortical modulation of transmission in spinal reflex pathways of man. *The Journal of physiology* **455,** 425-446.

Koshland GF & Smith JL. (1989). Mutable and immutable features of paw-shake responses after hindlimb deafferentation in the cat. *Journal of neurophysiology* **62,** 162-173.

bioRxiv preprint doi: https://doi.org/10.1101/012583; this version posted December 12, 2014. The copyright holder for this preprint (which was not certified by peer review) is the author/funder, who has granted bioRxiv a license to display the preprint in perpetuity. It is made available under aCC-BY-NC-ND 4.0 International license.

Kozelj S & Baker SN. (2014). Different phase delays of peripheral input to primate motor cortex and spinal cord promote cancellation at physiological tremor frequencies. *J Neurophysiol* **111,** 2001-2016.

Lidierth M & Wall PD. (1996). Synchronous inherent oscillations of potentials within the rat lumbar spinal cord. *Neuroscience letters* **220,** 25-28.

Lippold OC. (1970). Oscillation in the stretch reflex arc and the origin of the rhythmical, 8-12 C-S component of physiological tremor. *The Journal of physiology* **206,** 359-382.

Manjarrez E, Rojas-Piloni JG, Jimenez I & Rudomin P. (2000). Modulation of synaptic transmission from segmental afferents by spontaneous activity of dorsal horn spinal neurones in the cat. *J Physiol* **529 Pt 2,** 445-460.

Marsden CD, Meadows JC, Lange GW & Watson RS. (1969). The role of the ballistocardiac impulse in the genesis of physiological tremor. *Brain : a journal of neurology* **92,** 647-662.

Meunier S & Pierrot-Deseilligny E. (1998). Cortical control of presynaptic inhibition of Ia afferents in humans. *Exp Brain Res* **119,** 415-426.

Mitchell WK, Baker MR & Baker SN. (2007). Muscle responses to transcranial stimulation in man depend on background oscillatory activity. *The Journal of physiology* **583,** 567-579.

Rudomin P, Jimenez I, Solodkin M & Duenas S. (1983). Sites of action of segmental and descending control of transmission on pathways mediating PAD of Ia- and Ib-afferent fibers in cat spinal cord. *J Neurophysiol* **50,** 743-769.

Rudomin P, Solodkin M & Jimenez I. (1986). PAD and PAH response patterns of group Ia- and Ib-fibers to cutaneous and descending inputs in the cat spinal cord. *J Neurophysiol* **56,** 987-1006.

Salenius S, Portin K, Kajola M, Salmelin R & Hari R. (1997). Cortical control of human motoneuron firing during isometric contraction. *Journal of neurophysiology* **77,** 3401-3405.

Seki K, Perlmutter SI & Fetz EE. (2003). Sensory input to primate spinal cord is presynaptically inhibited during voluntary movement. *Nat Neurosci* **6,** 1309-1316.

bioRxiv preprint doi: https://doi.org/10.1101/012583; this version posted December 12, 2014. The copyright holder for this preprint (which was not certified by peer review) is the author/funder, who has granted bioRxiv a license to display the preprint in perpetuity. It is made available under aCC-BY-NC-ND 4.0 International license.

Seki K, Perlmutter SI & Fetz EE. (2009). Task-dependent modulation of primary afferent depolarization in cervical spinal cord of monkeys performing an instructed delay task. *J Neurophysiol* **102,** 85-99.

Soteropoulos DS, Williams ER & Baker SN. (2012). Cells in the monkey ponto-medullary reticular formation modulate their activity with slow finger movements. *J Physiol* **590,** 4011-4027.

Stuart D, Ott K, Ishikawa K & Eldred E. (1966). The rhythm of shivering. 3. Central contributions. *American journal of physical medicine* **45,** 91-104.

Vallbo AB & Wessberg J. (1993). Organization of motor output in slow finger movements in man. *J Physiol* **469,** 673-691.

Wall PD. (1958). Excitability changes in afferent fibre terminations and their relation to slow potentials. *J Physiol* **142,** 1-21.

Williams ER & Baker SN. (2009). Renshaw cell recurrent inhibition improves physiological tremor by reducing corticomuscular coupling at 10 Hz. *J Neurosci* **29,** 6616-6624.

Williams ER, Soteropoulos DS & Baker SN. (2009). Coherence between motor cortical activity and peripheral discontinuities during slow finger movements. *J Neurophysiol* **102,** 1296-1309.

Williams ER, Soteropoulos DS & Baker SN. (2010). Spinal interneuron circuits reduce approximately 10-Hz movement discontinuities by phase cancellation. *Proceedings of the National Academy of Sciences* **107,** 11098-11103.

bioRxiv preprint doi: https://doi.org/10.1101/012583; this version posted December 12, 2014. The copyright holder for this preprint (which was not certified by peer review) is the author/funder, who has granted bioRxiv a license to display the preprint in perpetuity. It is made available under aCC-BY-NC-ND 4.0 International license.

FIGURES AND LEGENDS

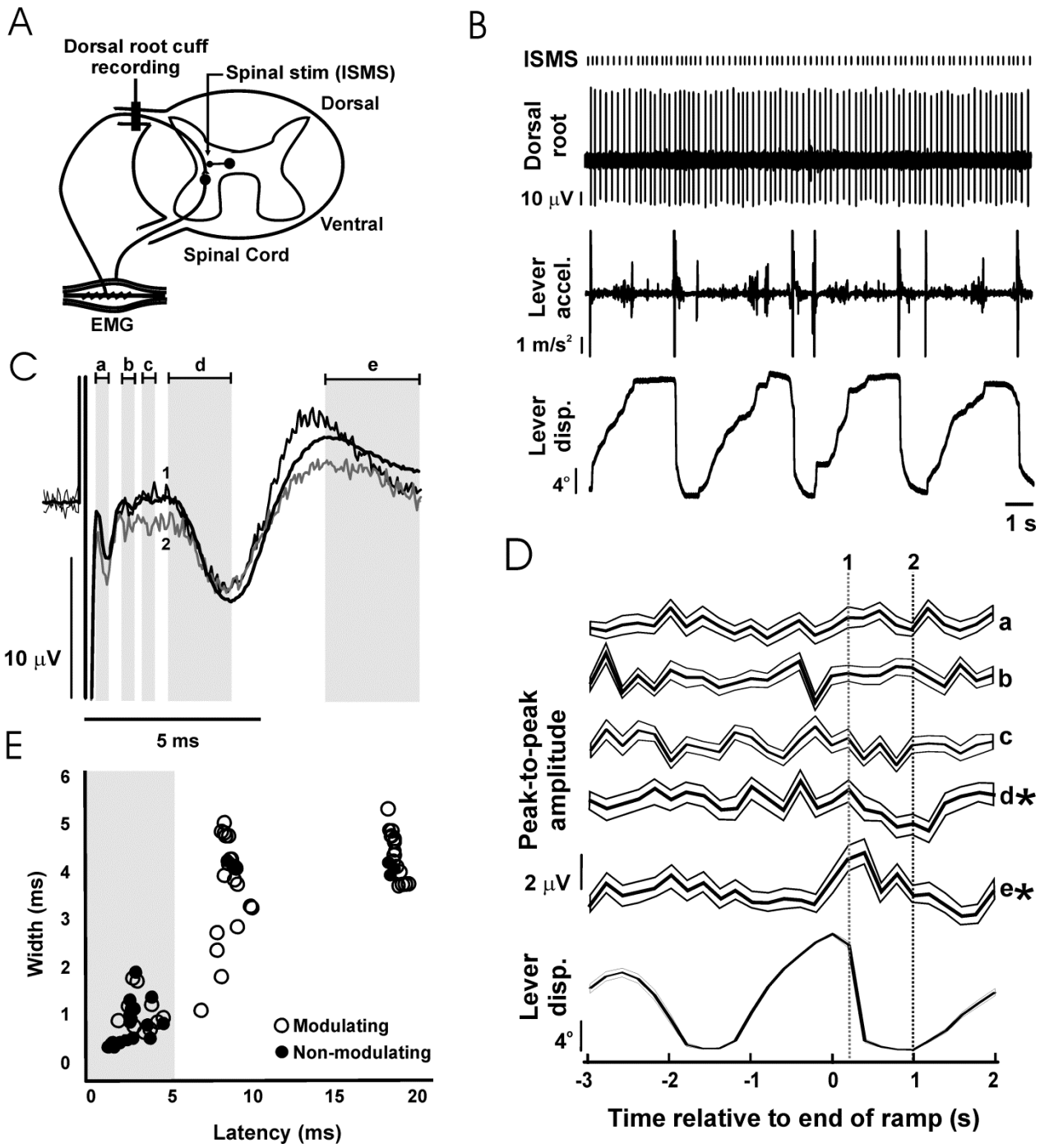

bioRxiv preprint doi: https://doi.org/10.1101/012583; this version posted December 12, 2014. The copyright holder for this preprint (which was not certified by peer review) is the author/funder, who has granted bioRxiv a license to display the preprint in perpetuity. It is made available under aCC-BY-NC-ND 4.0 International license.

Figure 1: Dorsal root potentials evoked by intra-spinal micro-stimulation (ISMS). A, schematic of the recording setup. A bipolar cuff electrode was implanted on the C8 or T1 dorsal root adjacent to the spinal cord. During task performance, ISMS was delivered at a location which elicited antidromic responses in the mixed population of afferents recorded at the dorsal root electrode. B, example raw data during task performance. C, example of responses evoked at the dorsal root by ISMS to a single spinal site (65 μA). Thick black trace represents grand-average (n=4080 stimuli); thin black and thin grey traces represent sub-averages from task-dependent bins marked by dotted lines in (D). Grey shading and lower case letters indicate different response components. D, task-dependent modulation of the responses indicated by lower case letters in (C). Each trace shows the mean response, with faint surrounding traces indicating the SEM. Traces are aligned to the end of the ramp phase of the task; average lever displacement is shown below in the same timeframe for comparison. Asterisks denote responses with significant task-dependent modulation. Vertical lines indicate times used to compute sub-averages illustrated in (C). E, scatter plot of the width versus latency of responses (n=88). Only responses with latency shorter than 5 ms (grey shading) were used in subsequent analysis (n=41).

bioRxiv preprint doi: https://doi.org/10.1101/012583; this version posted December 12, 2014. The copyright holder for this preprint (which was not certified by peer review) is the author/funder, who has granted bioRxiv a license to display the preprint in perpetuity. It is made available under aCC-BY-NC-ND 4.0 International license.

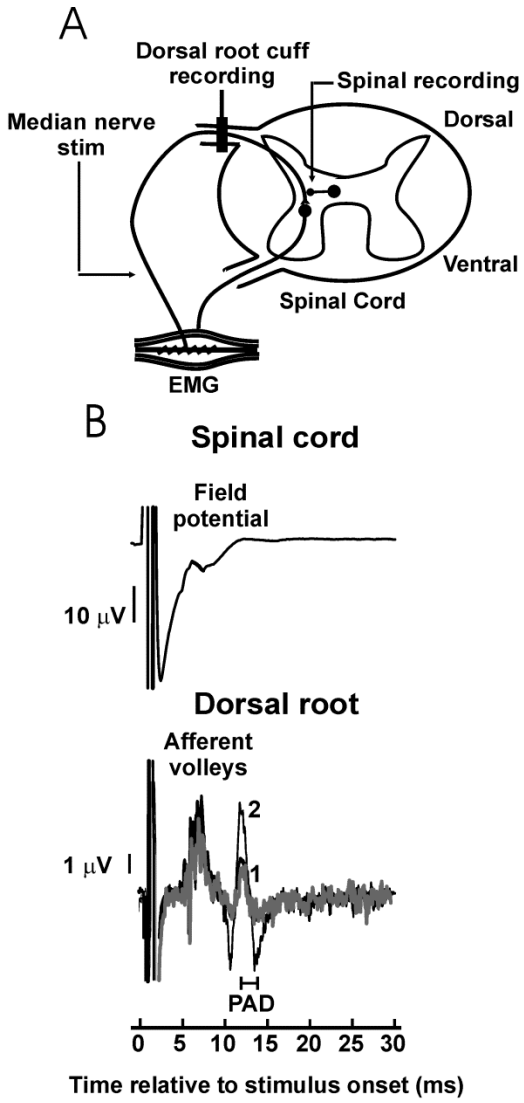

bioRxiv preprint doi: https://doi.org/10.1101/012583; this version posted December 12, 2014. The copyright holder for this preprint (which was not certified by peer review) is the author/funder, who has granted bioRxiv a license to display the preprint in perpetuity. It is made available under aCC-BY-NC-ND 4.0 International license.

Figure 2: Primary afferent depolarisation evoked by peripheral nerve stimulation. A, during task performance the median nerve was stimulated whilst recordings were made from the dorsal root and the spinal cord. B, example of averaged responses in one experiment. In the dorsal root potential, an early afferent volley is followed by later primary afferent depolarisation potential (PAD). Thick black trace represent grand-average (n=10859 stimuli), thin black and grey traces represent sub-averages from the times indicated in (C). C, significant task-dependent modulation of the amplitude of the PAD potential shown in (B). Top trace is mean PAD amplitude (thick line) and its SEM (thin line). Bottom trace is the average lever displacement, in the same timeframe, for reference. Vertical dotted lines indicate time points used for the corresponding coloured sub-averages in (B).

bioRxiv preprint doi: https://doi.org/10.1101/012583; this version posted December 12, 2014. The copyright holder for this preprint (which was not certified by peer review) is the author/funder, who has granted bioRxiv a license to display the preprint in perpetuity. It is made available under aCC-BY-NC-ND 4.0 International license.

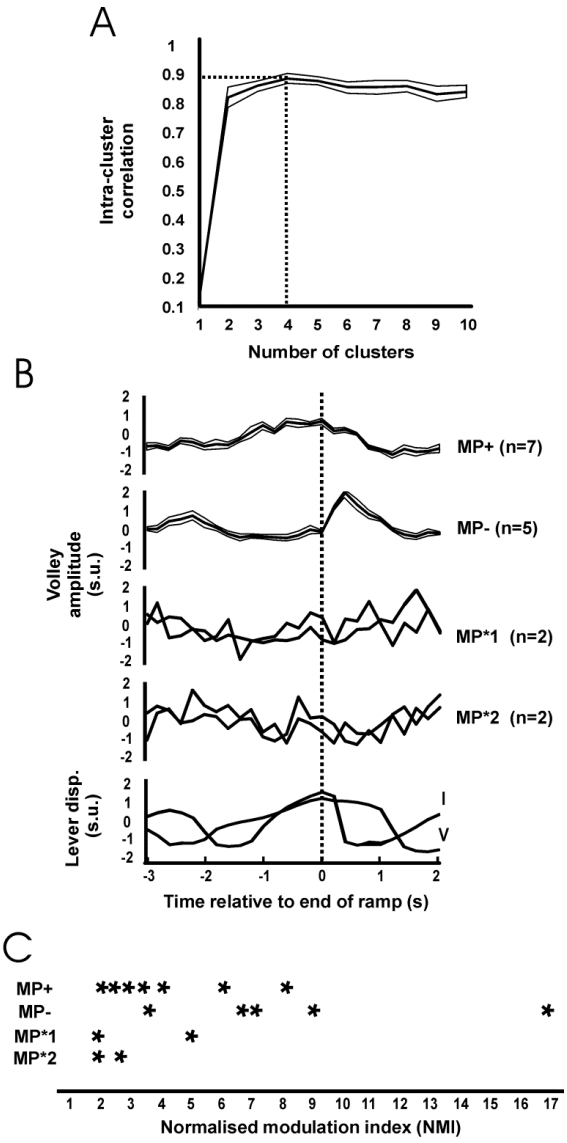

Figure 3: Clustering the patterns of task-dependent modulation. A, intra-cluster correlation (ICC, shown as mean ± SEM) as a function of the number of clusters. Maximum ICC was with 4 cluster (dotted lines). B, mean ± SEM (thick lines and associated thin lines) of the four modulating patterns identified from all 16 significantly modulating responses. Traces are aligned relative to the end of the ramp phase of the task. Beneath are shown averaged lever displacement traces for each monkey in the same timeframe, for comparison. In monkey I the ramp lasted 1 s, in monkey V it lasted 2 s. All traces have been normalised to have zero mean and unit standard deviation (standard units). C, normalised modulation index of significantly modulating responses, separated by cluster class.

bioRxiv preprint doi: https://doi.org/10.1101/012583; this version posted December 12, 2014. The copyright holder for this preprint (which was not certified by peer review) is the author/funder, who has granted bioRxiv a license to display the preprint in perpetuity. It is made available under aCC-BY-NC-ND 4.0 International license.

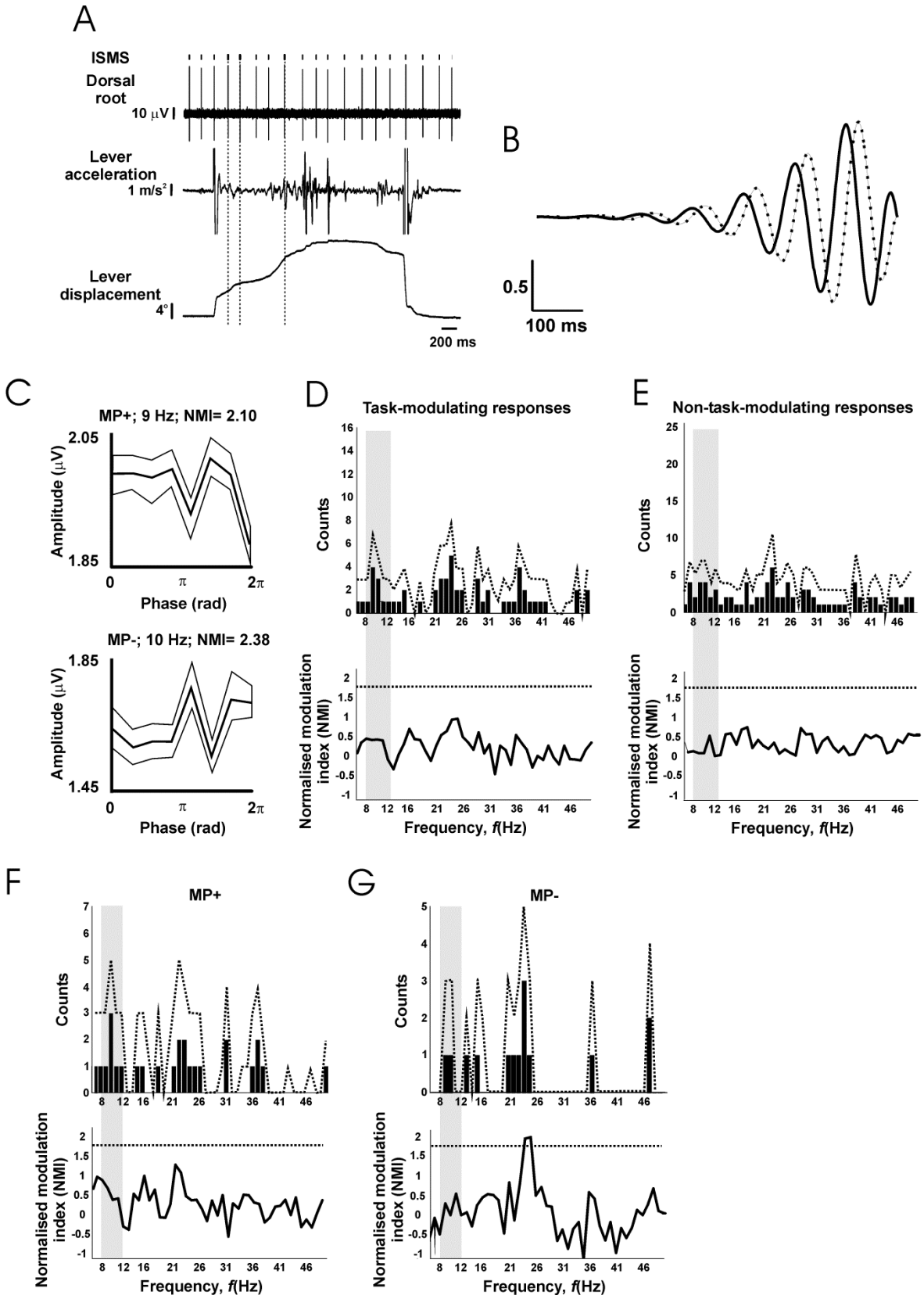

bioRxiv preprint doi: https://doi.org/10.1101/012583; this version posted December 12, 2014. The copyright holder for this preprint (which was not certified by peer review) is the author/funder, who has granted bioRxiv a license to display the preprint in perpetuity. It is made available under aCC-BY-NC-ND 4.0 International license.

Figure 4: Lack of tremor-dependent modulation. A, example raw data during task performance. Vertical dotted lines indicate stimuli which passed the criteria for inclusion in analysis of tremor modulation (lever velocity>15 °/s, lever acceleration power spectral peak in the 8-12 Hz range). B, asymmetric wavelet used to determine phase of oscillations in lever acceleration; both real (solid) and imaginary (dotted) components are shown. C, example tremor modulation profiles of responses categorised on the basis of their task modulation as MP+ or MP-. Each trace shows the mean (thick line) and SEM (thin lines) of the response amplitude as a function of oscillation phase. D, number of responses which showed significant modulation with phase, as a function of frequency (top), and the mean normalised modulation index (NMI, bottom), for responses with a significant task-dependent modulation. E, as (D), but for responses without significant task-dependent modulation. F, G, as (D), but only for responses categorised as MP+ (F) or MP- (G) on the basis of their task-dependent modulation. In D-G, dotted lines indicate significance limits; traces must cross these to achieve significance ($P<0.05$) for an individual bin. Grey shading indicates the 8-12 Hz range relevant to peripheral tremor.